Palaeontologia Electronica
palaeo-electronica.org

Cranial anatomy of *Indohyus indirae* (Raoellidae), an artiodactyl from the Eocene of India, and its implications for raoellid biology

Sonam Patel, Avinash C. Nanda, Maëva Orliac, and Johannes G.M. Thewissen

ABSTRACT

The raoellid artiodactyl *Indohyus indirae* is known from northern Pakistan and northwestern India, with substantial skeletal material found in the Sindkhatudi locality near Kalakot in Kashmir. Eight specimens from this locality, two of which exhibit deciduous dentitions, offer invaluable insights into cranial osteology of *Indohyus indirae*. We present a comprehensive examination of the cranial osteology of *Indohyus*, highlighting detailed unique features using this material. These specimens, though flattened dorsoventrally and mediolaterally, allow for anatomical observations. Previous literature has extensively employed these specimens for phylogenetic analyses indicating that *Indohyus* is a close relative of cetaceans. These findings are partly based on the material described here. Notably, the cranial morphology of *Indohyus* differs in several aspects from that of most early and middle Eocene artiodactyls. For instance, the rostrum of *Indohyus* is longer than that of most middle Eocene artiodactyls, resembling Eocene cetaceans. The positioning of the nasal opening above the incisors is similar to terrestrial artiodactyls. However, the ventral wall of the nasopharyngeal duct does not extend to the ear region, which distinguishes it from Eocene cetaceans. Moreover, the frontal bone is thick and has a concave profile, forming a dorsal shield for the laterally facing orbits. Furthermore, the tympanic bone has an involucrum, a feature that characterizes all cetaceans. These cranial features may be indicative of specific cranial functions and, given their similarity in some regards to Eocene cetaceans, could be related to the land-to-water transition. Further research, including explicit functional studies, is required to investigate these hypotheses.

Sonam Patel. Department of Anatomy and Neurobiology, Northeast Ohio Medical University, Rootstown, Ohio 44272, U.S.A. spatel37@neomed.edu
Avinash C. Nanda. Ranga Rao-Obergfell Trust for Geosciences, Dehradun, India.
Maeva Orliac. Institut des Sciences de l'Evolution, Montpellier, France. maeva.orliac@umontpellier.fr
Johannes G.M. Thewissen. Department of Anatomy and Neurobiology, Northeast Ohio Medical University, Rootstown, Ohio 44272, U.S.A (corresponding author) thewisse@neomed.edu

Final citation: Patel, Sonam, Nanda, Avinash C., Orliac, Maëva, and Thewissen, Johannes G.M. 2024. Cranial anatomy of *Indohyus indirae* (Raoellidae), an artiodactyl from the Eocene of India, and its implications for raoellid biology. Palaeontologia Electronica, 27(1):a21.
https://doi.org/10.26879/1307
palaeo-electronica.org/content/2024/5187-cranial-anatomy-of-indohyus

Keywords: *Indohyus*; Cetacea; Eocene; skull anatomy

Submission: 19 May 2023. Acceptance: 27 March 2024.

INTRODUCTION

Indohyus is a fox-sized raoellid artiodactyl from the Eocene of northwestern India and northern Pakistan (Ranga Rao, 1971; Sahni and Khare, 1972; Sahni et al., 1981; Thewissen et al., 2007; Orliac and Ducrocq, 2011; Rana et al., 2021). Much of the anatomy of *Indohyus* has been described, including the postcranial skeleton (Cooper et al., 2011), dentition (Thewissen et al., 2020), cranial endocast (Orliac and Thewissen, 2021), tooth wear patterns (Thewissen et al., 2011), middle ear (Mourlam, 2019) and dental eruption sequence (Rodrigues et al., 2019).

The phylogenetic relationships of cetaceans have been widely debated in the literature (e.g., Geisler and Uhen, 2005; O'Leary and Gatesy, 2007; Uhen et al., 2011; Gatesy et al., 2013; McGowen et al., 2014; Mourlam, 2019; Gohar et al., 2021). *Indohyus* has been included in a number of these, and it, or the family it represents, has been found to be the sister clade to cetaceans (Gatesy et al., 2013; McGowen et al., 2014; Mourlam, 2019). Images of the skull of *Indohyus* have been included in some papers (Thewissen et al., 2007, 2009, 2020; Thewissen, 2019), but no comprehensive description of cranial anatomy has been published. In light of this gap, the goals of this study are to describe the cranial anatomy of *Indohyus indirae* and discuss possible implications for its biology. As such, this study can form a foundation for future phylogenetic and functional studies.

The basic taxonomy and distribution of *Indohyus* were reviewed by Thewissen et al. (2020). The majority of fossils of *Indohyus,* including all specimens described here, were found at the Sindhkatudi locality, in rocks attributed to the Subathu Formation of northern India (synonym of the Kalakot Locality of Russell and Zhai, 1987). This formation encompasses different lithologies, and varies from red, to black, to green/purple in color. Being in the foreland of the Himalayas, these fossils have been severely deformed (Ranga Rao, 1971). The Sindhkatudi locality was discovered by Mr. Anne Ranga Rao near the village of Kalakot in Indian Jammu and Kashmir (locality description in Russell and Zhai, 1987), close to the line-of-control with Pakistani-held Kashmir. However, due to the tenuous security situation, Ranga Rao moved truckloads of blocks from the locality to Dehra Dun, and then extracted a small number of fossils from these blocks. Following Ranga Rao's unexpected death in 1999, his widow, Dr. Friedlinde Obergfell, safeguarded the collection as part of the Rangarao-Obergfell Trust for Geosciences (Thewissen, 2019). Eventually, she allowed one of us (J.G.M. Thewissen) access to the collection, and publications followed, mostly after her passing in 2007.

MATERIAL AND METHODS

The current description is based on specimens catalogued under the acronym RR (Ranga Rao Collection) and housed at the Ranga Rao-Obergfell Trust for Geosciences in Dehra Dun, India. These specimens were extracted from sediment by Dr. Richard Conley of Northeast Ohio Medical University. The study is based on several specimens of *Indohyus indirae*, each providing specific insights into the cranial anatomy and related features. RR 601 is a dorsoventrally crushed skull lacking the premaxilla and occiput and with no details of the orbito-temporal region preserved (Figure 1A-B). RR 207 is a dorsoventrally crushed skull, lacking the premaxilla and with few details of the orbito-temporal region preserved (Figure 1C-D), but with all molars and most premolars in situ. RR 208 (Figure 2A-B) is an obliquely medio-laterally crushed skull lacking its premaxilla and with few details of the orbito-temporal region. RR 209 is an obliquely medio-laterally crushed skull fragment that includes the caudal palatal regions housing premolars and molars, the orbits, and a part of the jugal arch (Figure 2C). RR 602 is a dorsoventrally crushed rostrum featuring a complete premaxilla, a partial maxilla, a complete nasal opening, and several teeth (Figure 3A-B). RR 210 is a skull fragment with the left ear region, mandibular fossa, occipital condyle, and a part of the occiput (Figure 3C). RR 262 is a fragmentary juvenile skull with deciduous teeth and partial medio-lateral and dorso-ventral crushing. It is attached to the lower jaw of a different individual, but partially retains the ear region (Figure 3D). RR 528 is a medio-laterally crushed rostrum of a juvenile with several deciduous and unerupted teeth. Three of these specimens (RR 207, 208, and 601) were CT-scanned under the supervision of one of us (Orliac)

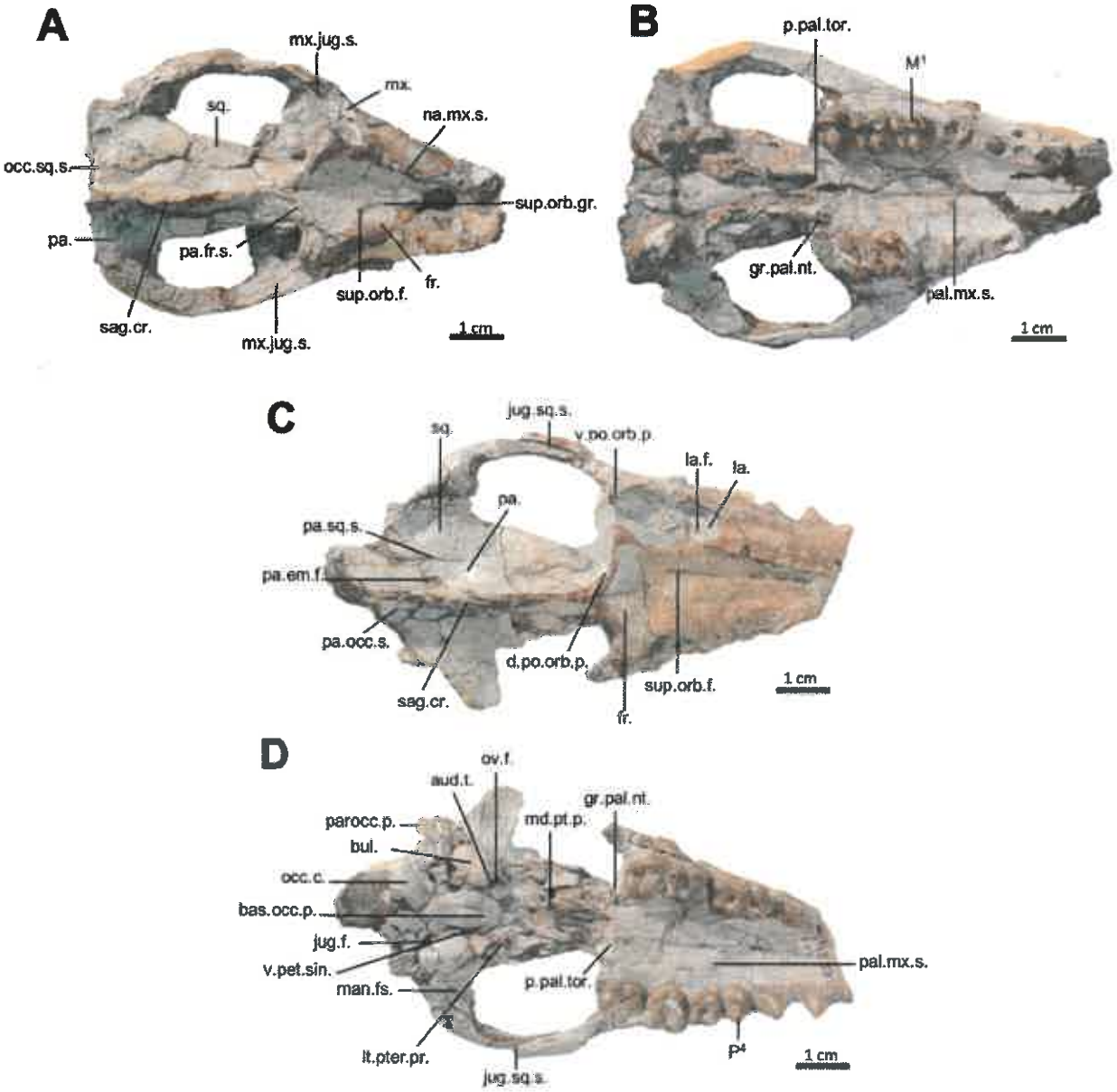

FIGURE 1. Cranial anatomy of *Indohyus indirae*. **A**, skull, dorsal view (RR 601). **B**, skull, ventral view (RR 601). **C**, skull, dorsal view (RR 207). **D**, skull, ventral view (RR 207).

at the Institut de Sciences de l'Evolution in Montpellier (Figures 4, 5). The methodology employed for these scans is comprehensively detailed in the work of Orliac and Thewissen (2021). The 3D data acquisition was performed at the µ-CT scanner facility of the Montpellier Rio Imaging platform (MRI) using an EasyTom 150 µ-CT scanner. Segmentation was performed using Avizo ® 9.3 (Thermo Fisher Scientific-FEI) to virtually excise the residual matrix. The reconstructions depicted in Figure 6 are based on the CT scans. Measurements of the cranial specimens of *Indohyus* are provided in Table 1. For a summary of dental measurements, see Thewissen et al. (2020).

Anatomical abbreviations. ant.pal.f., anterior palatine foramen; aud.t., auditory tube; bas.occ., basioccipital; bas.occ.p., process of basioccipital bone; bas.sph., basisphenoid; bul., bulla; coch., cochlea; d.po.orb.p., dorsal supraorbital process; e.a.m., external auditory meatus; f.mag., foramen magnum; fr., frontal; gr.pal.nt., greater palatine notch; hy.f., hypoglossal foramen; inv., involucrum; i.orb.f., infraorbital foramen; jug.ar., jugal arch; jug.sq.s., jugo-squamosal suture; la., lacrimal; la.f.,

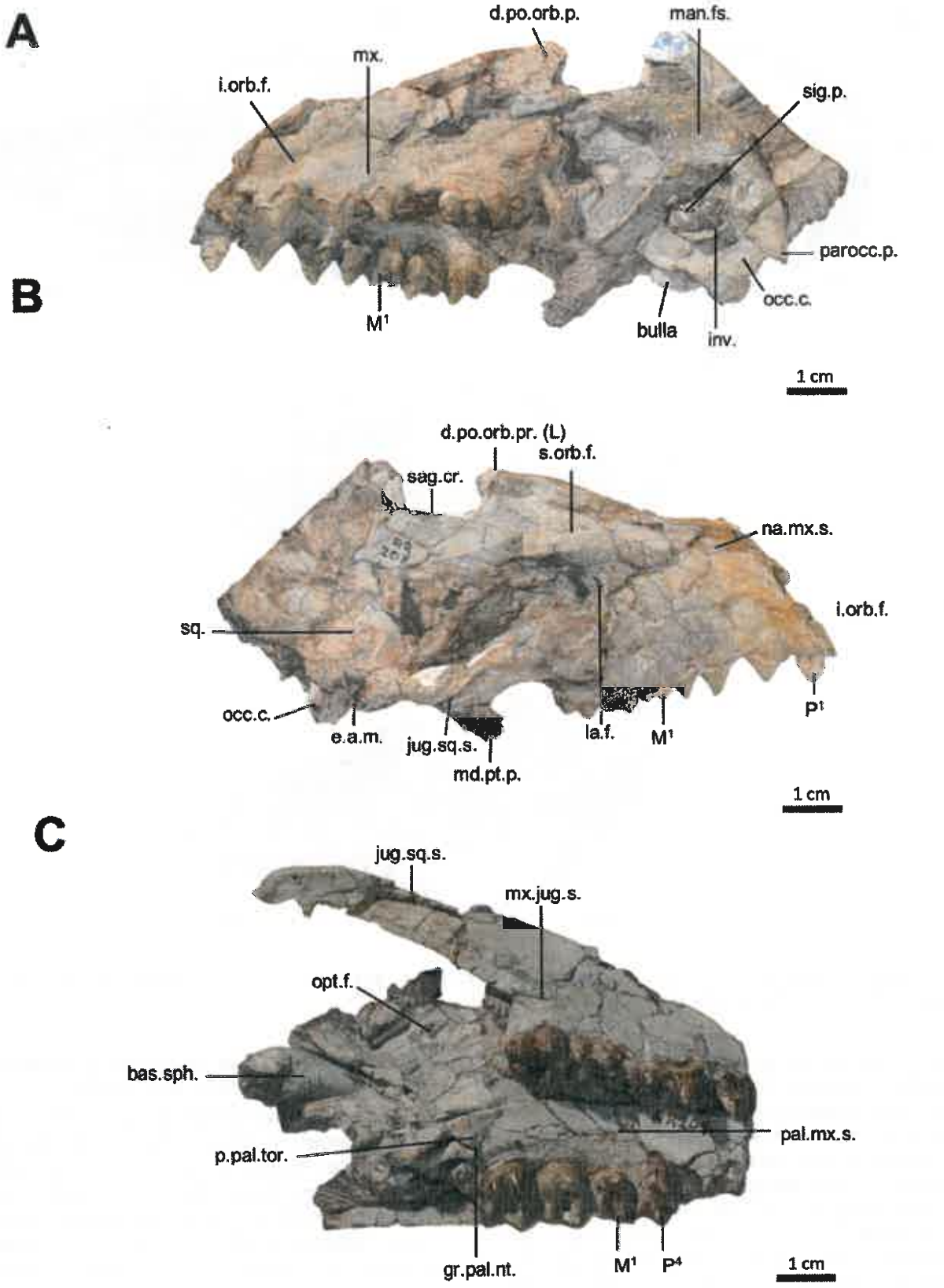

FIGURE 2. Cranial anatomy of *Indohyus indirae*. **A**, skull, left lateral view (RR 208). **B**, skull, right lateral view (RR 208). **C**, Oblique, ventral view (RR 209). For abbreviations see text.

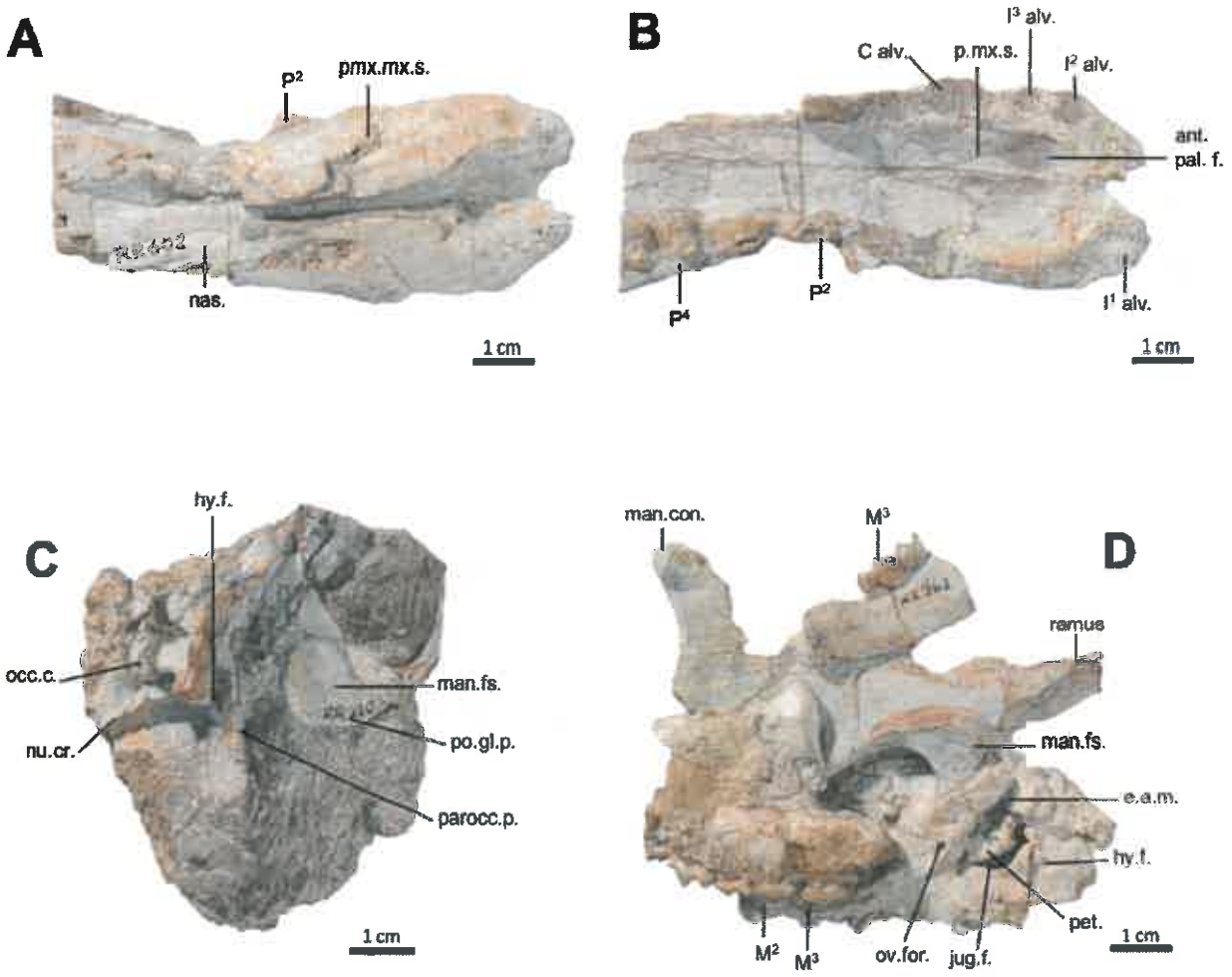

FIGURE 3. Cranial anatomy of *Indohyus indirae*. **A**, rostrum, dorsal view (RR 602). **B**, rostrum, ventral view (RR 602). **C**, Basicranium (RR 210). **D**, Juvenile skull with unassociated lower jaw (RR 262).

lacrimal foramen; lt.pter.pr., lateral pterygoid process; man.fs., mandibular fossa; mx., maxilla; mx.jug.s., maxillo-jugal suture; med.cr., median crest; md.pt.pr., medial pterygoid process; md.pt.p., medial pterygoid process; nas., nasal; na.mx.s., naso-maxillary suture; nas.se., nasal septum; nu.cr., nuchal crest; occ.c., occipital condyle; occ.sq.s., occipitosquamosal suture; olf. chamber, olfactory chamber; opt.f., optic foramen; ov.f., oval foramen; pal., palatine; pal.mx.s., palato-maxillary suture; pa., parietal; pa.em.f., parietal emissary foramen; pa.fr.s., parieto-frontal suture; parocc.p., paroccipital process; pa.occ.s., parieto-occipital suture; pa.sq.s., parietosquamosal suture; p.g.p., postglenoid process; pmx.mx.s., premaxilla-maxilla suture; po.gl.p., postglenoid process; po.orb.p., postorbital process; p.pal.tor., postpalatine torus; sag.cr., sagittal crest; sig.s., sigmoid sinus; sq., squamosal; sup.orb.ca., supraorbital canal; sup.orb.gr., supraorbital groove; sup.orb.f., supraorbital foramen; tr.sin, transverse sinus; turb., turbinate; v.nas.gr., vomeronasal groove; v.po.orb.p., ventral postorbital process; v.pet.s.f., foramen for ventral petrosal sinus.

DESCRIPTION

Premaxilla. The premaxilla of *Indohyus* is long and narrow (Figure 3A-B). With the three incisor alveoli arranged mostly in a rostro-caudal direction (I^{1-3} alv., a lateral view of premaxilla RR 331 was published by Thewissen et al., 2020: fig. 14.1 f-g. The alveolus for I^2 is the largest of the three but is smaller than the canine alveolus. The alveolus of C^1 is situated on the suture between the premaxilla and the maxilla. On the palate, this suture extends medio-rostrally from the anterior margin of the canine alveolus to the anterior palatine foramen (Figure 3A-B; ant.pal.f.). From the foramen, the

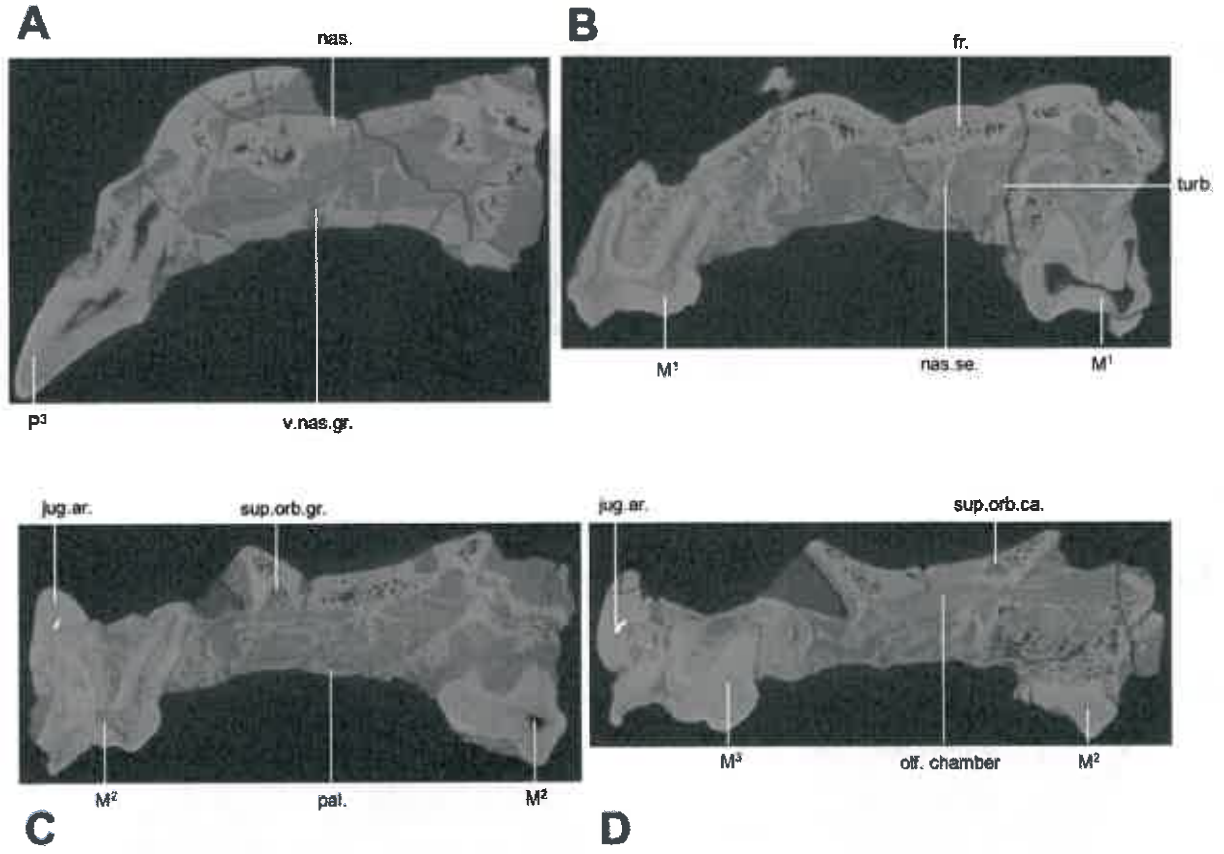

FIGURE 4. Annotated CT slices highlighting the cranial anatomy of *Indohyus indirae* (RR207), featuring detailed transverse sections of the skull. A, slice 403. B, slice 817. C, slice 1043. D, slice 1180.

premaxilla-maxilla suture (pmx.mx.s.) extends medio-caudally to the median plane at the level of the canine. On the lateral side of the rostrum, the premaxilla-maxilla suture extends dorso-caudally to reach the nasal bones (RR 528).

Nasal. The nasal is long and slender and widens caudally, but its anterior most extension is not preserved (Figures 1A-B, 3A-B; nas.). The posterior edge of the nasal opening is dorsal to I^3 (Figure 3A-B). The widest point is dorsal to P^3, where the left and right naso-maxillary sutures (Figure 2A-B; na.mx.s.) converge to reach the median plane dorsal to P^3 or P^4 (RR 528).

Maxilla. The maxilla (mx.) makes up most of the palate, with the narrowest point occurring over P^2, an area of apparent weakness of the skull, as the region rostral to this point is missing in most specimens. On the palate, the maxilla has no diastemata caudal to the canine (Figure 3A-B). The suture between palatine and the maxilla (pal.mx.s.) extends rostrally from the palatal edge, with the left and right sutures converging near P^4 and meeting in the midline near P^3 (Figure 1A-D). The caudal edge of the palate is deeply indented by the greater palatine notch (Figure 1A-D; gr.pal.nt.). P^{1-3} are double-rooted, while P^4 and the upper molars are triple-rooted (Figure 1A-B). On the face, the infraorbital foramen is located dorsal to the area where P^2 and P^3 meet (Figure 1C-D; i.orb.f.). The suture between maxilla (mx.) and lacrimal (la.) extends from the nasal bone ventro-caudally to the rim of the orbit (Figure 2A-C). The maxilla contributes to the floor or the orbit, but laterally, the entire ventral edge of the orbit is formed by the jugal (Figure 1A-B). The ventral postorbital process is large, extending dorsally over one-third of the orbital length (Figure 2C). The maxilla forms the rostral part of this process, while the jugal bone forms the caudal part. Rostrally, the suture between maxilla and jugal reaches the lateral palatal edge over M^3 (Figures 1C-D, 2C; jug.mx.s.).

Lacrimal. The lacrimal has a square-shaped appearance on the face (RR 207; Figure 1; la.). The lacrimal foramen opens on the orbital side of the lacrimal (Figures 1C-D, 2A-B; la.f.), but details of the bone within the orbit are poorly preserved.

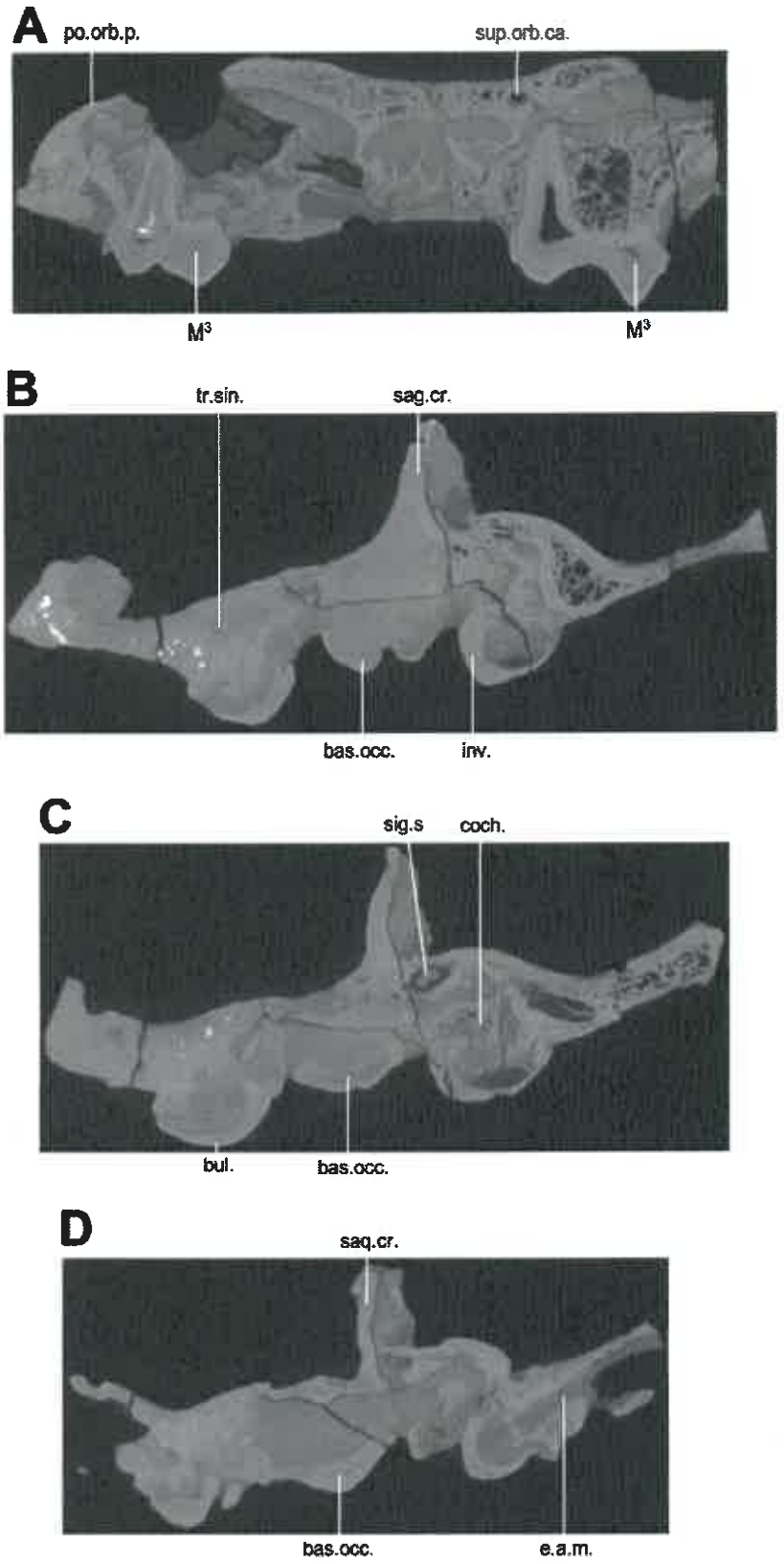

FIGURE 5. Annotated CT slices highlighting the cranial anatomy of *Indohyus indirae* (RR207), featuring detailed transverse sections of the skull. **A**, slice 1303. **B**, slice 2142. **C**, slice 2230. **D**, slice 2302.

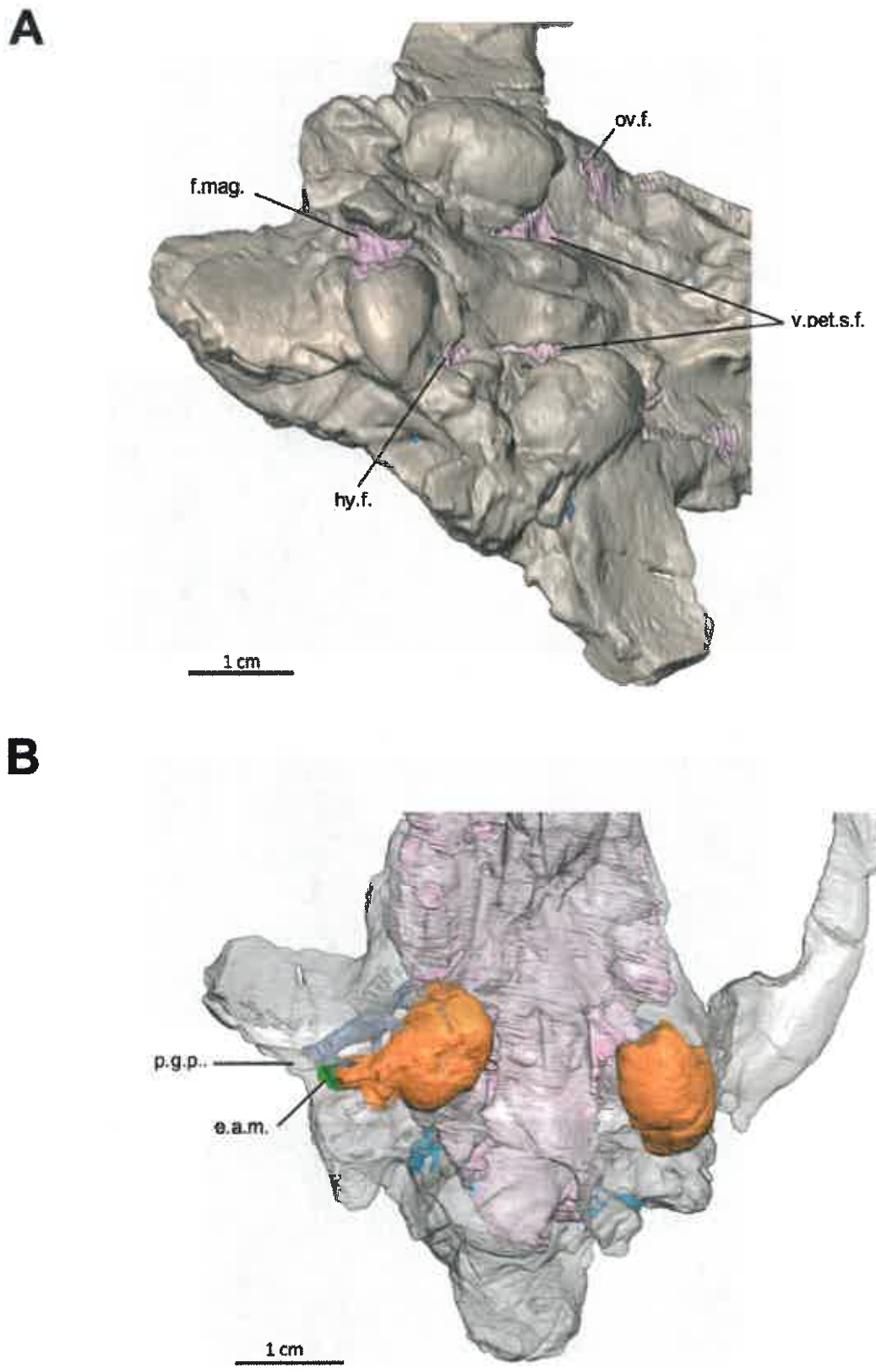

FIGURE 6. 3D rendering of the basicranium of *Indohyus indirae* in oblique (**A**) and ventral (**B**) views. In **A**, the foramina opening into the endocast are highlighted in pink. In **B**, the bullae are depicted in orange.

TABLE 1. Cranial measurement of *Indohyus indirae*. All measurements are parallel or perpendicular to the sagittal plane.

Specimen Number	Variable	Metric (mm)
RR 601	Maximum width across jugal arches	71.9
RR 601	Maximum width across lateral bullae	35.7
RR 601	Maximum length of the left bulla	14.8
RR 601	Maximum width of the left bulla	11.4
RR 601	Width of palate between medial side of M/3s	18.5
RR 208	Length from caudal side of C to caudal side of occipital condyle	126.6
RR 207	Length from caudal side of C to caudal side of occipital condyle	116.9
RR 207	Width of palate between medial side of M/3s	19.4
RR 207	Maximum width across lateral bullae	34.8
RR 207	Maximum width across lateral side of mandibular fossae	65.8
RR 207	Maximum length of left bulla	13.5
RR 207	Maximum width of left bulla	9.9
RR 207	Maximum width across occipital condyles	20.6
RR 602	Width of palate between medial side of Cs	18.7
RR 602	Length from rostrum to caudal side of canine	38.1

The suture between lacrimal (la.) and frontal (fr.) extends cranio-caudally, with the frontal overhanging the lacrimal to a certain extent (Figure 1A-B).

Jugal. The jugal bone makes up the caudal side of the ventral postorbital process (Figure 1C-D; v.p.orb.p), and forms most of the ventral orbital rim (Figures 1A-D, 2C). The jugal bone narrows caudally, terminating just rostral to the mandibular fossa (man.fs.). Throughout its length in the temporal fossa, the jugal bone has a long dorsal suture with the squamosal (Figure 1C-D; jug.sq.s.). This squamosal process tapers rostrally and constitutes the dorsal rim of the jugal arch.

Palatine. The posterior edge of the palate is indented by a deep greater palatine notch (Figure 1A-B; gr.pal.nt.). The postpalatine torus (p.pal.tor.) is prominent, extending laterally from the median plane, bending caudally at the greater palatine notch, and aligning with the thickened edge of the pterygoid process.

Sphenoid and pterygoid. The bony lateral walls of the nasopharyngeal duct have a distinct suture with the palatine at the postpalatine torus (Figure 2C). The dorsal aspect of the nasopharyngeal duct bears a median crest that partially divides the duct into left and right sides (Figure 1A-B; med.cr.) Caudally, this wall divides into a pronounced medial pterygoid process (Figure 1C-D; md.pt.p.) and a weaker lateral pterygoid process (Figure 1A-B; lt.pter.pr.). The lateral pterygoid process continues as a slight crest to the lateral side of the bulla, with the oval foramen located just lateral to this crest (Figure 3D; ov.f.) and partly covered, in ventral view, by the bulla (Figure 1C-D). The suture between basioccipital and basisphenoid is obliterated in most specimens, but visible in a juvenile (RR 209; Figure 2C). This suture is located near the cranial extent of the bullae.

Frontal. The frontal (fr.) is thick and medio-laterally concave (Figures 1A-D, 2A-B). It forms the sharp dorsal edge of the orbit, and the rostral part of the dorsal supraorbital process (d.p.orb.p.). The suture with the parietal runs along the caudal edge of the dorsal supraorbital process (Figure 1A-D; pa.fr.s.). There is a distinct supraorbital foramen (Figure 1C-D; sup.orb.f.), accompanied by a prominent groove (Figure 1A-B; sup.orb.gr.) extending rostrally from it.

Parietal. The dorsal and lateral sides of the braincase are formed by the parietals, and these form a cone-shape that tapers rostrally up to the frontal shield. From the postorbital process, the suture between parietal (pa.) and frontal (fr.) runs along the temporal crest (Figure 1A-B; pa.fr.s.). Left and right temporal crests join in the median plane to form the sagittal crest (sag.cr.), which continues caudally and crosses the suture between parietal and occipital (Figure 1C-D; pa.occ.s.). This suture is at the base of the nuchal shield. The suture between squamosal and parietal reaches approximately halfway up the braincase (Figure 1A-D; pa.sq.s.). A prominent parietal emissary foramen is

situated dorsal to this suture in RR 207 (pa.em.f.) and located close to the sagittal crest in RR 601 (Orliac and Thewissen, 2021).

Occipital. The occipital forms the nuchal shield, with prominent nuchal crests (Figure 3C; nu.cr.). The shield extends well beyond the occipital condyles, forming an inverted U-shape in the caudal view (Figures 1C-D, 2A-B, 3C). The central part of the occipital extends over the dorsal edge of the foramen magnum. The occipital condyles face equally ventral and caudal and form two-thirds of the lateral edge of the foramen magnum (Figure 1C-D; occ.c.). The exoccipital forms a prominent paroccipital process (Figure 2A-B; parocc.p.), which is triangular and flat, shielding the ear region in caudal view (Figure 1C-D). The hypoglossal foramen is located just rostral to the occipital condyle on its ventral side (Figure 3C-D; hy.f.). Although the condylar foramen remains invisible, a trace of its vein was identified by Orliac and Thewissen (2021) based on CT scans. The basioccipital bears bilateral prominences at the level of the cranial extent of the bullae (Figure 1A-D; bas.occ.p.).

Squamosal. The squamosal forms the lateral part of the braincase and, in this area, articulates with frontal, parietal, and occipital (Figures 1A-B, 2A-B, 3C; sq.). On the lateral aspect of the skull, the occipito-squamosal suture (Figure 1A-B; occ.sq.s.) extends rostrally from the nuchal crest. Laterally, the squamosal contributes to the jugal arch, with its suture (Figure 2A-B; jug.sq.s.) crossing the jugal arch obliquely. The caudal side of the postglenoid process of the squamosal (Figure 1A-B; po.gl.p.) is indented by the external auditory meatus (e.a.m.) and bears a wide postglenoid foramen. The mandibular fossa (Figures 1A-D, 3C; man.fs.) is extensive and flat, located immediately adjacent to the lateral surface of the bulla. The postglenoid process (Figures 1A-B, 3C; po.gl.p.) is small and triangular.

Ectotympanic. The ectotympanic forms a prominent bulla that shares sutures with occipital, squamosal, and sphenoid (Figure 1A-D). Mediocaudally, the bulla bears a groove that likely housed the first segment of the hyoid in life. The jugular foramen is located in the area where this groove touches the occipital (Figure 1C-D; jug.f.). Medial to the bulla, a small part of the petrosal is exposed, situated laterally to the basioccipital. A long and narrow foramen for the ventral petrosal sinus separates these two bones (Figure 1C-D; v.pet.s.). In a juvenile specimen (RR 262; Figure 3D) with the bulla is missing, the jugular foramen is connected to the foramen for the ventral petrosal sinus. Rostro-medially, the bulla is indented, bearing a foramen for the auditory tube (Figure 1C-D; aud.t.). Laterally, the bulla is immediately adjacent to the mandibular fossa, with the joint surface of the latter extends ventrally making a broad contact with the bulla (Figure 1C-D). The medial part of the bulla is developed into the involucrum (Figure 2A-B; inv.), and part of the sigmoid process is visible on a fractured surface (Figure 2A-B; sig.p.). We omitted the description of the petrosal and the middle ear cavity in this paper, which was already covered by Mourlam (2019). The external auditory meatus indents the postglenoid process. Ventrally, the meatus is ossified over a short distance lateral to the bulla.

COMPARISON AND DISCUSSION

Length of the snout. The premaxilla of *Indohyus* is surprisingly long for an artiodactyl of this size. Although the premaxilla is not preserved as part of the entire skull in any specimen, combining measurements from different specimens (Table 1) estimate that the distance between the snout tip and posterior edge of the canine alveolus makes up one-quarter of the ventral skull length (Figures 2A-B, 3A-B). In comparison, the premaxilla in other early and middle Eocene artiodactyls (*Diacodexis* and *Helohyus*) is shorter. The length of the premaxilla in *Indohyus* is attributed to the alignment of the incisors in a rostral-caudal plane. The incisors are lined-up on a very gentle rostro-caudally arch in *Indohyus*, which is similar to pakicetid cetaceans (Thewissen and Hussain, 1998) and some middle Eocene artiodactyls (*Gujaratia;* Russell et al., 1983). However, the arch is more pronounced, and thus the anterior palate broader in other artiodactyls. It has been hypothesized as a synapomorphy of raoellids and cetaceans (Geisler and Uhen, 2005). It is suggested that the long premaxilla in *Indohyus* is related to feeding, similar to small, modern artiodactyls (Dubost, 1975). Isotopic evidence indicates that *Indohyus* was an herbivore (Thewissen et al., 2007), as can be expected for an early artiodactyl, (*Messelobunodon*; Richter, 1981). However, its tooth wear suggests that oral processing of the food resembled cetaceans, even though those are carnivorous (Thewissen et al., 2011). The dentition of *Indohyus* also resembles that of *Pakicetid* cetaceans in the relative size of P^4, which has a higher crown (in the labial view) than the upper molars (Thewissen and Hussain, 1998; Thewissen et al., 2020). These proportions are common in Eocene cetaceans. The diet of *Indo-*

hyus remains unclear and warrants further investigation, potentially utilizing stable isotype analysis and tooth wear studies.

Orbit size and position. Nummela et al. (2006) described the position and size of the orbits in Eocene cetaceans. They found that these characteristics vary between families. Protocetids and basilosaurids have large eyes that face laterally and are located under a thick supraorbital shield. On the other hand, the orbits of *Ambulocetus* were also large, but they were located close together and dorsal on the skull while facing laterally. We speculate that this has implications for feeding behavior. It is likely that *Ambulocetus* was not exclusively hunting underwater but was also spying prey while most of its body was submerged. *Remingtonocetus* has small eyes that faced laterally. Its eyes were of less importance, given that it lived in muddy water (Thewissen and Bajpai, 2009), and had large middle ears, and prey detection might have been based on acoustic clues. Its relative *Andrewsiphius* also had small eyes; these are located dorsally but face laterally (Thewissen and Bajpai, 2009). In pakicetids, the eyes are close to the midline with a narrow interorbital region, but their eyes face more dorsal than lateral, suggesting that pakicetids hunted prey that was not submerged. Meanwhile, the orbits of *Indohyus* are similar to those of other early and middle Eocene artiodactyls and they face laterally, as in terrestrial artiodactyls (Thewissen et al., 2007). Stable isotopes and skeletal histology (Thewissen et al., 2007) suggest that *Indohyus* spent considerable time in the water. However, given that it was not a predator, the position of its eyes did not relate to food gathering.

Frontal shape. A surprising feature of *Indohyus* is the shape and position of the frontal bone. The frontal is concave medio-laterally, giving rise to a distinct depression just rostral to the nuchal temporal crests. This feature is also present and even more distinct in pakicetid cetaceans, where it has been related to the dorsal convergence of the eyes (Nummela et al., 2006). However, orbital convergence in *Indohyus* is much smaller than in pakicetids. The frontal has a concave profile rostrally in certain Oligocene artiodactyls, such as *Leptomeryx* and *Poebrotherium* (Scott, 1940), but it is convex caudally, presumably marking the presence of the olfactory bulb deep to it. The olfactory bulb in *Indohyus* is small (Orliac and Thewissen, 2021), consistent with the concave, and very thick frontal which overlies it, and consistent with the small olfactory bulb in pakicetid cetaceans (Kishida et al., 2015).

Middle ear and hearing. Mourlam (2019) described the middle and inner ear of *Indohyus*, with a specific interest in determining the frequencies that the ears were tuned to. Thewissen et al. (2007) noted that *Indohyus* had a thickened medial bullar wall, a feature often used to diagnose cetaceans (Gatesy et al., 2013), and referred to as an involucrum in cetaceans. The function of the cetacean involucrum has been related to bone-conducted hearing, which is important in species that live in dense media (water) or whose head is in contact with dense media (soil) (Barklow, 2004; Nummela et al., 2007). In *Indohyus*, this feature can be taken as additional evidence of its transitional nature between living on land and living in water, supporting the aquatic adaptations suggested by limb bone histology (Cooper et al., 2011) and oxygen isotopes (Thewissen et al., 2007). Although ear ossicles are not known for *Indohyus*, it is known that even pakicetids have ear ossicles that are larger, and of a different shape from those of land mammals (Thewissen et al., 1993). Further discoveries of *Indohyus* fossils may resolve the question of whether its ossicles already show some of the changes that characterize later cetaceans.

Nasopharyngeal duct and hyoid bone. The nasopharyngeal duct and pterygoid region of *Indohyus* match those of terrestrial artiodactyls, unlike Eocene cetaceans. The bony palate does not extend beyond the last molars, whereas the nasopharyngeal duct in pakicetids and ambulocetids is ossified ventrally (Thewissen et al., 1996; Nummela et al., 2006). The lateral walls of the nasopharyngeal duct terminate well anterior to the ear region, whereas in Eocene cetaceans, they extend to the ear region. *Indohyus* retains a lateral pterygoid plate, unlike many modern artiodactyls and Eocene cetaceans (Nummela et al., 2006; Thewissen and Bajpai, 2009). *Indohyus* and Eocene cetaceans have a similar extensive ventrally projecting medial pterygoid process, unlike modern artiodactyls (Getty, 1975). It is likely that throat morphology changed significantly in the land to water transition, possibly to adapt to new types of food and feeding. However, a detailed study into the functional aspects of each of these changes is needed.

CONCLUSIONS

The skull of *Indohyus* has offered a plethora of features that have been used to study the phylogenetic position of the clade. It shows a combination

of features that are common in terrestrial artiodactyls, Eocene cetaceans, as well as younger, aquatic cetaceans. These findings underscore the critical initial steps taken towards aquatic adaptation. The functional analysis of the skull of *Indohyus* is still in its early stages. Much of cranial design will be impacted by the evolution toward aquatic behaviors in general or aquatic adaptations of specific members of the cetacean clade. The position of the nares, the size and position of the orbits, the nasopharyngeal duct, the middle and inner ear, the length and position of the snout, the shape of the teeth, and the size and orientation of the temporal fossae all interact and affect skull morphology and are related to the function of the sense organs (vision, olfaction, hearing), food acquisition and processing, and breathing. Studying the evolution of these organs and comparing them to terrestrial relatives and Eocene cetaceans will further elucidate cetacean evolution.

ACKNOWLEDGEMENTS

We acknowledge the contribution of Mr. A.R. Rao and Dr. F. Obergfell for collecting and curating these specimens. We thank the trustees of the Obergfell-Ranga Rao Trust of Geosciences for allowing us to study these specimens and Dr. R. Conley for preparation of the fossils. This research was supported by the National Science Foundation (grant to J.T.) and the Hennecke Family Foundation.

REFERENCES

Barklow, W.E. 2004. Amphibious communication with sound in hippos, *Hippopotamus amphibius*. Animal Behavior, 68:1125–1132. https://doi.org/10.1016/j.anbehav.2003.10.034

Cooper, L.N., Thewissen, J.G.M., Bajpai, S., and Tiwari, B.N. 2011. Postcranial morphology and locomotion of the Eocene raoellid *Indohyus* (Artiodactyla: Mammalia). Historical Biology, 24:279–310. https://doi.org/10.1080/08912963.2011.624184

Dubost, G. 1975. Le comportement du chevrotain africain, *Hyemoschus aquaticus* Ogilby (Artiodactyla, Ruminantia). Sa signification écologique et phylogénétique. Zeitschrift für Tierpsychologie, 37:449–501. https://doi.org/10.1111/j.1439-0310.1975.tb00889.x

Gatesy, J., Geisler, J.H., Chang, J., Buell, C., Berta, A., Meredith, R.W., Springer, M.S., and McGowen, M.R. 2013. A phylogenetic blueprint for a modern whale. Molecular Phylogenetics and Evolution, 66:479–506. https://doi.org/10.1016/j.ympev.2012.10.012

Geisler, J.H. and Uhen, M.D. 2005 Phylogenetic Relationships of Extinct Cetartiodactyls: Results of Simultaneous Analyses of Molecular, Morphological, and Stratigraphic Data, 12:145–160. https://doi.org/10.1007/s10914-005-4963-8

Getty, R. 1975. Sisson and Grossman's The Anatomy of the Domestic Animals. W.B. Saunders Company, Philadelphia. https://doi.org/10.5962/bhl.title.68343

Gohar, S.A., Antar, M., and Boessenecker, R.W. 2021. A new protocetid whale offers clues to biogeography and feeding ecology in early cetacean evolution. Proceedings of the Royal Society B, 288:20211368. https://doi.org/10.1098/rspb.2021.1368

Kishida, T., Thewissen, J.G.M., and Hayakawa, T. 2015. Aquatic adaptation and the evolution of smell and taste in whales. Zoological Letters, 1:9. https://doi.org/10.1186/s40851-014-0002-z

McGowen, M.R., Gatesy, J., and Wildman, D.E. 2014. Molecular evolution tracks macroevolutionary transitions in Cetacea. Trends in Ecology & Evolution, 29:336–346. https://doi.org/10.1016/j.tree.2014.04.001

Mourlam, M. 2019. Région auditive des artiodactyles: signal phylogénétique et écologique. Unpublished PhD Thesis, Université de Montpellier, Montpellier, France.

Nummela, S., Hussain, S.T., and Thewissen, J.G.M. 2006. Cranial anatomy of Pakicetidae (Cetacea, Mammalia). Journal of Vertebrate Paleontology, 26:746–759. https://doi.org/10.1671/0272-4634(2006)26[746:CAOPCM]2.0.CO;2

O'Leary, M.A. and Gatesy, J. 2007. Impact of increased character sampling on the phylogeny of Cetartiodactyla (Mammalia): combined analysis including fossils. Cladistics, 24:397–442. https://doi.org/10.1111/j.1096-0031.2007.00187.x

Orliac, M. J. and Ducrocq, S. 2011. Eocene raoellids (Mammalia, Cetartiodactyla) outside the Indian subcontinent: palaeogeographical implications. Geological Magazine, 149:1–13. https://doi.org/10.1017/S0016756811000586

Orliac, M.J. and Thewissen, J.G.M. 2021. The endocranial cast of *Indohyus* (Artiodactyla, Raoellidae): the origin of the cetacean brain. Journal of Mammalian Evolution, 28:831–843. https://doi.org/10.1007/s10914-021-09552-x

Ranga Rao, A. 1971. New mammals from Murree (Kalakot Zone) of the Himalayan foot hills near Kalakot, Jammu & Kashmir State, India. Journal of the Geological Society of India, 12:125–134.

Rana, R.S., Waqas, M., Orliac, M., Folie, A., and Smith, T. 2021. A new basal raoellid artiodactyl (Mammalia) from the middle Eocene Subathu Group of Rajouri District, Jammu and Kashmir, northwest Himalaya, India. Geobios, 66-67:193–206. https://doi.org/10.1016/j.geobios.2020.12.003

Richter, G.1981. Untersuchungen zur Ernährung von *Messelobunodon schaeferi* (Mammalia, Artiodactyla). Senckenbergiana Lethaea, 61:355–370.

Rodrigues, H.G., Lihoreau, F., Orliac, M.J., Thewissen, J.G.M., and Boisserie, J.R. 2019. Unexpected evolutionary patterns of dental ontogenetic traits in cetartiodactyl mammals. Proceedings of the Royal Society B, 193:413–431. https://doi.org/10.1098/rspb.2018.2417

Russell, D.E., Thewissen, J.G.M., and Sigogneau-Russell, D. 1983. A new artiodactyl (Mammalia) from the Eocene of North-West Pakistan. Part II: Cranial osteology. Proceedings of the Koninklijke Nederlandse Akademie voor Wetenschappen, Series B, 86:285–300.

Russell, D.E. and Zhai, R. 1987. The Paleogene of Asia: mammals and stratigraphy. Mémoires du Muséum National d'Histoire Naturelle C, 52:1–488.

Sahni, A. and Khare, S.K. 1972 (for 1971). Three new Eocene mammals from Rajauri District, Jammu and Kashmir. Journal of the Palaeontological Society of India, 16:41–53.

Sahni, A., Bhatia, S.B., Hartenberger, J.L., Jaeger, J.-J., Kumar, K., Sudre, J., and Vianey-Liaud, M. 1981. Vertebrates from the Subathu formation and comments on the biogeography of Indian subcontinent during the Early Paleogene. Bulletin de la Société Géologique de France, 23:68–695. https://doi.org/10.2113/gssgfbull.S7-XXIII.6.689

Scott, W.B. 1940. The Mammalian Fauna of the White River Oligocene, Part 4: Artiodactyla. Transactions of the American Philosophical Society, 5:775822. https://doi.org/10.2307/1005504

Thewissen, J.G.M. 2019. The Walking Whales: From Land to Water in Eight Million Years. University of California Press, Berkeley, California. https://doi.org/10.3375/043.040.0412

Thewissen, J.G.M., Madar, S.I., and Hussain, S.T. 1996. *Ambulocetus natans*, an Eocene cetacean (Mammalia) from Pakistan. Courier Forschungsinstitut Senckenberg, 190:1–86.

Thewissen, J.G.M., Cooper, L.N., Clementz, M.T., Bajpai, S., and Tiwari, B.N. 2007. Whales originated from aquatic artiodactyls in the Eocene epoch of India. Nature, 450:1190–1194.

Thewissen, J.G.M. and Bajpai, S. 2009. New skeletal material of *Andrewsiphius* and *Kutchicetus*, two Eocene cetaceans from India. Journal of Paleontology, 83:635–663. https://doi.org/10.1666/08-045.1

Thewissen, J.G.M., Cooper, L.N., George, J.C., and Bajpai, S. 2009. From land to water: the origin of whales, dolphins, and porpoises. Evolution: Education and Outreach, 2:272–288. https://doi.org/10.1007/s12052-009-0135-2

Thewissen, J.G.M., Sensor, J.D., Clementz, M.T., and Bajpai, S. 2011. Evolution of dental wear and diet during the origin of whales. Paleobiology, 37:655–669. https://doi.org./10.1666/10038.1

Thewissen, J.G.M., Nanda, A.C., and Bajpai, S. 2020. *Indohyus*, endemic radiation of raoellid artiodactyls in the Eocene of India and Pakistan, p. 337–346. In Prasad, G.V. and Patnaik, R. (eds.), Biological Consequences of Plate Tectonics, Vertebrate Paleobiology and

Paleoanthropology. Springer, Cham.
https://doi.org/10.1007/978-3-030-49753-8_14
Uhen, M.D., Pyenson, N.D., Devries, T.J., Urbina, M., and Renne, P.R. 2011. New Middle Eocene Whales from the Pisco Basin of Peru. Journal of Paleontology, 85:955--969.
https://www.jstor.org/stable/23020145